

Temperature dependence of magnetic excitations in singlet-ground-state systems. II. Excited-state spin waves near the Curie temperature in Pr₃Tl

W. J. L. Buyers, T. M. Holden, and A. Perreault*

Atomic Energy of Canada Limited, Chalk River, Ontario, Canada

(Received 15 July 1974)

A theory has been developed of the temperature dependence of the spin waves in a system involving transitions between all levels of the ground multiplet of an ion. The excitations out of both ground and excited states are described by the product of annihilation and creation operators for the single-ion states of the crystalline field and molecular field. The spin-waves are obtained with the random-phase approximation applied to the interlevel transition operators rather than to S_z as in conventional spin-wave theory. Numerical results have been obtained for Pr₃Tl that agree with the neutron measurements of Birgeneau and coworkers. There is little variation with temperature through the phase transition of the scattering from modes having wave vectors greater than $(0.25, 0.25, 0)2\pi/a$. This is partly because the measurements average over two groups of spin waves that interact, the spin waves out of the ground state and the excited-state spin waves corresponding to the $\Gamma_4 \rightarrow \Gamma_3$ transition. The $\Gamma_1 - \Gamma_4$ zone-center modes are strongly temperature dependent but do not go soft. They decrease in frequency as T rises from zero to T_C by factors of ~ 4 and ~ 6 for S_+ and S_- modes, respectively. Very-low-frequency transverse (S_+) modes (~ 0.02 THz) appear at elevated temperatures and do go soft as $T \rightarrow T_C$. These modes correspond to transitions between the states of the weakly exchange-split Γ_4 triplet.

I. INTRODUCTION

A large number of attempts have been made to understand the varied and often surprising magnetic properties of singlet-ground-state systems.¹⁻³ The simplest theory of such systems is the singlet-singlet model⁴ in which the excited states of the lowest multiplet are approximated by a single level. This theory, when solved within the random-phase approximation, predicts that the frequency of the longitudinal zone-center spin-wave mode will fall to zero as the temperature is raised from zero to the transition temperature, and will then rise again and tend to the crystal-field splitting, Δ , as $T \rightarrow \infty$. The behavior of the modes as observed experimentally is in marked contrast to this. The neutron scattering results on single-crystal TbSb (Ref. 5) show that as $T \rightarrow T_N$ the mode falls in frequency concurrently with the growth of critical scattering centered on zero frequency. Above T_N there is no evidence of a well-defined excitation. In Pr₃Tl, on the other hand, the frequency of the neutron peak observed in the polycrystal^{6,7} remains well defined and almost independent of temperature through T_C . It was not clear from these measurements, which had to be made at nonzero wave vectors because the specimen was polycrystalline, whether the zone-center mode does or does not go soft.

A refinement of the theory, the singlet-triplet model, is not in significantly better agreement with experiment. In this model four states of the ground multiplet are included, the singlet ground state, Γ_1 , and a triplet excited state, Γ_4 , as found for Tb³⁺ and Pr³⁺.

In the model of Pink⁸ the magnetic dipole transitions between the singlet and the outer members of the triplet are ignored as is the moment carried by the triplet states and thus the model is not applicable to Pr₃Tl. Hsieh and Blume⁹ applied the singlet-triplet model to TbSb. They found the Goldstone mode that Birgeneau⁷ has suggested should always occur²⁴ in the singlet-triplet model, but it is this feature of the model that is responsible for most of the disagreement with the experimental results which show a large energy gap.⁵ Smith,¹⁰ who has developed the singlet-triplet model for Pr compounds and included all singlet to triplet transitions, found that near T_C the modes within the triplet prevent the $\Gamma_4 - \Gamma_1$ modes from going soft.

The only theories of singlet-ground-state systems in which the real level scheme has been included are the pseudoboson theories of Holden *et al.*⁵ for TbSb and Cooper¹¹ for Pr₃Tl. The pseudoboson theory^{12,13} is restricted to $T=0$ since transitions are included out of the ground state only. It was found that the wave-vector-dependent exchange mixing of the higher-frequency transitions into the lowest spin-wave branches introduced an energy gap at $\vec{q}=0$. No model, therefore, that ignores the true level structure can provide a realistic description of the spin waves, in particular the singlet-triplet model with its Goldstone mode.

The pseudoboson theory is a zero-temperature theory and cannot readily be extended to finite temperatures in a many-level system where the pure-spin Holstein-Primakov transformation is no longer applicable. Thus it has not been possible until

now to calculate the temperature dependence of the spin-wave spectrum in real many-level systems. The many-level structure is important in TbSb (Ref. 5), Pr₃Tl (Ref. 7), and in earlier studies of KCoF₃ (Ref. 13) and CoF₂ (Ref. 14) where the ground state of the magnetic ion is degenerate. A theory of the temperature dependence of spin waves that can be applied to both singlet- and degenerate-ground-state systems is clearly required. Such a theory is developed in this paper and applied to Pr₃Tl.

To describe the spin waves we abandon the pseudoboson concept and work with the basic operators that annihilate and create a given single-ion state. The single-ion states are those of the crystal field and molecular field. Products of these describe the transitions between all states of the ground multiplet and not just those out of the ground state as in the pseudoboson theory. There is thus one set of spin waves out of each level of the ground multiplet and these are coupled together by the exchange interaction if they have the same symmetry. The theory therefore includes the mode-mode interaction that occurs at finite temperature in Pr₃Tl between the spin waves out of the ground state and those out of the excited states. This interaction is absent in most theories to date. The singlet-triplet model of Smith¹⁰ does of course contain the interaction of the modes within the triplet with the $\Gamma_4 - \Gamma_1$ modes, but the interaction with the excited-state $\Gamma_3 - \Gamma_4$ modes is ignored. The latter interaction is necessary if the neutron scattering results are to be understood.

In Sec. II the dynamical susceptibility theory is developed. It is shown in Sec. III that the theory is equivalent in the $T=0$ limit to pseudoboson theory, and in the paramagnetic phase to the theory of Fulde and Peschel,¹⁵ and that it has the same form as the theory of spin waves in itinerant magnets. Some of the results for the paramagnetic phase of Pr₃Tl were obtained by the present authors in a previous paper to be referred to as Paper I.¹⁶ In this paper we have used the theory generalized to be valid in the ferromagnetic as well as the paramagnetic phase and the numerical results are presented in Sec. IV. Comparison is made with the experiments of Birgeneau *et al.*,^{6,7} and the nature of the soft mode and the mode-mode interaction is discussed.

II. GENERALIZED DYNAMICAL SUSCEPTIBILITY

A. Properties of the single-ion Hamiltonian

The Hamiltonian for spin waves in a crystal containing rare-earth ions of total angular momentum (orbital plus spin) \vec{S} coupled by isotropic exchange and subjected to a crystalline electric field is

$$\mathcal{H} = \sum_i \mathcal{H}_{cf}(i) + \sum_{ij} J(ij) \vec{S}(i) \cdot \vec{S}(j). \quad (1)$$

This may be divided into a single-ion part

$$\mathcal{H}_1 = \sum_i \mathcal{H}_{cf}(i) + \sum_i S_z(i) \left(2 \sum_j J(ij) \langle S_z(j) \rangle \right) \quad (2)$$

and an interion part

$$\begin{aligned} \mathcal{H}_2 = & \sum_{ij} J(ij) S_z(i) [S_z(j) - 2 \langle S_z(j) \rangle] \\ & + \frac{1}{2} \sum_{ij} J(ij) [S_+(i) S_-(j) + S_-(i) S_+(j)]. \end{aligned} \quad (3)$$

The single-ion part, since \mathcal{H}_{cf} is a known function of \vec{S} in terms of a sum of operator equivalents,¹⁷ O_n^m , is first diagonalized exactly for a given molecular field

$$H_{mf} = 2 \sum_j J(ij) \langle S_z(j) \rangle \quad (4)$$

to give a set of eigenfunctions, $|n\rangle$, and eigenvalues, ω_n , satisfying

$$\mathcal{H} |n\rangle = \omega_n |n\rangle. \quad (5)$$

The states $|n\rangle$ are a linear combination of the basic spin states $|S_z=S\rangle$ to $|S_z=-S\rangle$. Matrix elements of any component of the spin, S_z , S_+ , and S_- in practice, are then computed between all $(2S+1)$ levels of the ground multiplet. [The case of a transition-metal ion with $(2S+1) \times (2l+1)$ levels can also be treated. \mathcal{H}_{cf} is then the sum of the spin-orbit interaction and the noncubic part of the crystal field and \vec{S} is the pure spin.] The average spin may be calculated from

$$\langle S_z \rangle = \sum_n S_{znn} f_n, \quad (6)$$

where

$$f_n = \exp(-\omega_n/k_B T) / \left(\sum_m \exp(-\omega_m/k_B T) \right) \quad (7)$$

and

$$S_{znn} = \langle n | S_z | n \rangle.$$

This value of $\langle S_z \rangle$ is then substituted in Eq. (4) and the process repeated until $\langle S_z \rangle$ and hence the eigenfunctions and eigenvalues have achieved self-consistency. This is the molecular field or best single-ion approximation. Numerical results obtained from this procedure applied to Pr₃Tl are given in Table I and Fig. 1 of Paper I and Fig. 4 of the present paper.

The single-ion Hamiltonian may now be written

$$\mathcal{H}_1 = \sum_i \sum_n \omega_n C_n^\dagger(i) C_n(i). \quad (8)$$

The operator C_n annihilates the state $|n\rangle$. Within all $2S+1$ states of the ground multiplet a complete description of \vec{S} is given by the projections

$$\begin{aligned}
S_+ &= \sum_{mn} S_{+mn} C_m^\dagger C_n, \\
S_- &= \sum_{mn} S_{-mn} C_m^\dagger C_n, \\
S_z &= \sum_{mn} S_{zmn} C_m^\dagger C_n,
\end{aligned} \tag{9}$$

where

$$S_{\alpha mn} = \langle m | S_\alpha | n \rangle. \tag{10}$$

The coefficients of the expansion of \vec{S} are the matrix elements of \vec{S} evaluated between the single-ion states $|n\rangle$. This description of \vec{S} is exact within the ground multiplet to the extent that the high-energy excited spin-orbit states can be neglected. It is easily verified with the aid of the property of annihilation operators

$$[C_m, C_n^\dagger]_z = \delta_{mn}, \tag{11}$$

that the projection (9) preserves as it must the spin commutation relations

$$\vec{S} \times \vec{S} = i\vec{S}, \tag{12}$$

and that the transition operators satisfy

$$[C_m^\dagger C_n, C_r^\dagger C_s] = \delta_{mr} C_m^\dagger C_s - \delta_{sm} C_r^\dagger C_n \tag{13}$$

and

$$\sum_{rs} [C_m^\dagger C_n, C_r^\dagger C_s] S_{\alpha rs} = \sum_s (C_m^\dagger C_s S_{\alpha ns} - C_s^\dagger C_n S_{\alpha sm}), \tag{14}$$

where α may represent +, -, or z and a commutator without a sign external to the square bracket has a negative sign between its terms. The two signs of the commutator of Eq. (11) show that the statistics of the C_n operators is immaterial; Eqs. (12) and (13) are satisfied for either Bose "particles" (integral S) or Fermi "particles" (half-integral S).

Only some of the matrix elements of S_+ , S_- , and S_z between the levels $|n\rangle$ will be nonzero. Since the crystal-field operators O_n^m contain no terms with $m=1$ the matrix elements of the transverse components of spin are entirely nondiagonal

$$S_{+nn} = 0. \tag{15}$$

This does not mean that the longitudinal spin component of spin will be entirely diagonal for there are in general inelastic transitions governed by the nonzero values of S_{zmn} ($m \neq n$) which give rise to the Davydov excitations. For exchange of the Heisenberg or of the uniaxially anisotropic form ($J_z \neq J_x = J_y$) the excitations divide into pure longitudinal (Davydov) and pure transverse spin waves.

For ions in a sufficiently symmetric environment it is found that between the levels m and n , if any one of S_+ , S_- , or S_z has a nonzero matrix element, then the other two have zero matrix ele-

ments. Thus if

$$S_{+mn} \neq 0$$

then

$$S_{-mn} = 0 \tag{16}$$

and

$$S_{zmn} = 0.$$

This will be used to simplify the equation of motion for the spins and is valid for Tb^{3+} , Pr^{3+} , and Co^{2+} in a cubic or tetragonal field as in TbSb ,⁵ Pr_3Tl ,¹⁶ and KCoF_3 ,¹³ but not for a field with a rhombic distortion as in CoF_2 .¹⁸

B. Interion coupling and equation of motion

The total Hamiltonian is the sum of the single-ion part (8) and the interion part (3):

$$\begin{aligned}
\mathcal{H} &= \sum_i \sum_n \omega_n C_n^\dagger(i) C_n(i) \\
&+ \sum_{ij} J(ij) S_z(i) [S_z(j) - 2\langle S_z(j) \rangle] \\
&+ \frac{1}{2} \sum_{ij} J(ij) [S_+(i) S_-(j) + S_-(i) S_+(j)].
\end{aligned} \tag{17}$$

The spin components are given in terms of the C_n operators by Eq. (9). The spin-wave spectrum and neutron scattering can be obtained from the dynamical susceptibility. In the magnetically ordered phase of a cubic system the susceptibility is anisotropic and has a transverse part

$$\begin{aligned}
G^{+-}(ij, t) &\equiv G(S_+(i), S_-(j), t) \\
&\equiv -i\Theta(t) \langle [S_+(i, t), S_-(j, 0)] \rangle
\end{aligned} \tag{18}$$

and a longitudinal part

$$G^{zz}(ij, t) \equiv -i\Theta(t) \langle [S_z(i, t), S_z(j, 0)] \rangle, \tag{19}$$

where $\Theta(t)$ is the unit step function. The following Fourier transforms are defined:

$$G(\vec{q}, t) = \frac{1}{N} \sum_i G(ij, t) e^{[i\vec{q} \cdot (\vec{r}_i - \vec{r}_j)]} \tag{20}$$

and

$$G(ij, \omega) = \int G(ij, t) e^{i\omega t} dt. \tag{21}$$

The Heisenberg equation of motion,

$$\omega G(A, B, \omega) = \langle [A, B] \rangle + G([A, \mathcal{H}], B, \omega), \tag{22}$$

may be applied to the transverse and longitudinal susceptibility in which A, B are S_+ , S_- or S_z , S_z , respectively, but it is better to define first an interlevel susceptibility \hat{G} by the equation

$$G^{\alpha\beta}(ij, \omega) \equiv \sum_{mn} S_{\alpha mn} \hat{G}^\beta(mn, ij, \omega), \tag{23}$$

where $\alpha, \beta = +, -, \text{ or } z$. The theory proceeds by

applying the equation of motion to \hat{G}^β in which $A = C_m^\dagger C_n$ and $B = S_\beta$. The decoupling is performed on \hat{G} and G is then recovered from Eq. (23).

The commutator with the Hamiltonian in (22) involves three types of terms in \mathcal{H} , the diagonal terms, the transverse terms, and the longitudinal terms. In obtaining an equation for \hat{G} the commu-

tator of $C_m^\dagger C_n$ with the diagonal terms gives

$$\sum_k \sum_r [C_m^\dagger(i)C_n(j), C_r^\dagger(k)C_r(k)]\omega_r = \delta_{ij}(\omega_n - \omega_m)C_m^\dagger(i)C_n(i). \quad (24)$$

The transverse terms give, with the aid of (14),

$$\begin{aligned} \sum_{kl} J_{kl} [C_m^\dagger(i)C_n(i), S_+(k)S_-(l)] &= \sum_l J_{il} \sum_s [S_{+ns}(i)C_m^\dagger(i)C_s(i) - S_{+sm}(i)C_s^\dagger(i)C_n(i)] \sum_{pq} S_{-qp}(l)C_q^\dagger(l)C_p(l) \\ &+ \sum_l J_{li} \sum_s [S_{-ns}(i)C_m^\dagger(i)C_s(i) - S_{-sm}(i)C_s^\dagger(i)C_n(i)] \sum_{pq} S_{+qp}(l)C_q^\dagger(l)C_p(l). \end{aligned} \quad (25)$$

In order to decouple the equations the random-phase decoupling is used:

$$C_m^\dagger(i)C_s(i)C_q^\dagger(l)C_p(l) = f_m(i)\delta_{ms}C_q^\dagger(l)C_p(l) + f_q(l)\delta_{pq}C_m^\dagger(i)C_s(i). \quad (26)$$

This decoupling is similar to that used in the band theory of magnetism (see Cooke,¹⁹ for example) where the subscripts are band indices. It is different from the usual random-phase-approximation (RPA) decoupling for magnetic systems, where S_z within a Green's function is replaced by $\langle S_z \rangle$, because it is applied in detail of each of the coupled equations for the interlevel transitions, mn , rather than to the equation for S_+ .

The decoupling (26) applied to the right-hand side of (25) gives four terms, two of which are zero because of (15) leaving

$$\sum_l J_{il} \left[S_{+nm}(f_m - f_n) \sum_{pq} S_{-qp} C_q^\dagger(l) C_p(l) \right.$$

$$\left. + S_{-nm}(f_m - f_n) \sum_{pq} S_{+qp} C_q^\dagger(l) C_p(l) \right] \quad (27)$$

as the total contribution from the transverse terms in the Hamiltonian. Since the single-ion levels are the same for all ions in a perfect crystal, the labels on the f_m and the matrix elements have been dropped.

The commutator of $C_m^\dagger(i)C_n(i)$ with the longitudinal terms in the Hamiltonian may be evaluated in a similar manner. The fluctuating terms on site i are found to cancel since they have already been included in the single-ion part of the Hamiltonian and the result is

$$\begin{aligned} \sum_{lk} J_{kl} [C_m^\dagger(i)C_n(i), S_z(k)\{S_z(l) - 2\langle S_z(l) \rangle\}] \\ = 2 \sum_l J_{il} S_{znm}(f_m - f_n) \sum_{pq} S_{zqp} C_q^\dagger(l) C_p(l). \end{aligned} \quad (28)$$

The final equation for the interlevel susceptibility is

$$\begin{aligned} \omega \hat{G}^\beta(mn, ij, \omega) &= (f_m - f_n) S_{\beta nm} \delta_{ij} + (\omega_n - \omega_m) \hat{G}^\beta(mn, ij, \omega) + \sum_l J_{il} \left[S_{+nm}(f_m - f_n) \sum_{pq} S_{-qp} \hat{G}^\beta(qp, lj, \omega) \right. \\ &\left. + S_{-nm}(f_m - f_n) \sum_{pq} S_{+qp} \hat{G}^\beta(qp, lj, \omega) \right] + 2 \sum_l J_{il} S_{znm}(f_m - f_n) \sum_{pq} S_{zqp} \hat{G}^\beta(qp, lj, \omega). \end{aligned} \quad (29)$$

The single-site dynamical susceptibility, $g^{\alpha\beta}(\vec{q}, \omega)$, is the solution for $J_{il} = 0$ in Eq. (29). In Fourier transforms, after multiplying through by $S_{\alpha mn}$, dividing by $\omega - \omega_n + \omega_m$ and summing mn , it is

$$g^{\alpha\beta}(\vec{q}, \omega) \equiv g^{\alpha\beta}(\omega) = \sum_{mn} \frac{S_{\alpha mn} S_{\beta nm} (f_m - f_n)}{\omega - \omega_n + \omega_m}. \quad (30)$$

By applying the same procedure to the full equation (29) it is found that

$$\begin{aligned} G^{\alpha\beta}(\vec{q}, \omega) &= g^{\alpha\beta}(\omega) + g^{\alpha+}(\omega) J(\vec{q}) G^{-\beta}(\vec{q}, \omega) \\ &+ g^{\alpha-}(\vec{q}, \omega) J(\vec{q}) G^{+\beta}(\vec{q}, \omega) \\ &+ 2g^{\alpha z}(\omega) J(\vec{q}) G^{z\beta}(\vec{q}, \omega). \end{aligned} \quad (31)$$

For the systems of interest in this paper where the matrix elements satisfy Eq. (16) the only non-zero components of the single-ion susceptibility (30) are g^{+-} , g^{-+} , or g^{zz} . The solution for the spin waves is then

$$G^{+-}(\vec{q}, \omega) = \frac{g^{+-}(\omega)}{1 - J(\vec{q})g^{+-}(\omega)} \quad (32)$$

for the transverse modes (the equation for G^{-+} is the same with $- \leftrightarrow +$), and

$$G^{zz}(\vec{q}, \omega) = \frac{g^{zz}(\omega)}{1 - 2J(\vec{q})g^{zz}(\omega)} \quad (33)$$

for the longitudinal modes. These equations are deceptively simple because most of the physics of the detailed level structure and matrix elements is contained within the temperature-dependent single-ion susceptibility (30). That such a simple form is possible is a reflection of the particular form of the isotropic interion coupling in exchange-coupled systems. Axially anisotropic exchange ($J_z \neq J_x = J_y$) can also be handled by evaluating $g(\omega)$ with J_z and then using in the renormalization J_x in (32) and J_z in (33).

The transition temperature is where the longitudinal susceptibility diverges:

$$1/g^{zz}(0) = 2J(\vec{0}) = 2zJ. \quad (34)$$

The $\omega \rightarrow 0$ limit of $g^{zz}(\omega)$ is not given correctly by the theory, however, since the quasielastic fluctuations are ignored in the RPA.²⁵ In practice, therefore, the transition temperature is found by raising T until $\langle S_z \rangle$, Eq. (6), falls to zero using the self-consistent single-ion states of Sec. IIA. This gives the molecular-field-theory transition temperature. The magnetization $\langle S_z \rangle$ is found to fall smoothly to zero as $T \rightarrow T_c$ in contrast to the first-order phase transition found in the singlet-singlet model.⁴

The neutron scattering $S(\vec{Q}, \omega)$ is directly related to the generalized susceptibility by

$$S(\vec{Q}, \omega) = \left(\frac{\gamma e^2}{2mc^2} \right)^2 f(\vec{Q})^2 (1 - e^{-\beta\omega})^{-1} \text{Im}G(\vec{Q}, \omega), \quad (35)$$

where

$$G(\vec{Q}, \omega) = \sum_{\alpha=x,y,z} (1 - \hat{Q}_\alpha^2) G^{\alpha\alpha}(\vec{Q}, \omega). \quad (36)$$

For polycrystalline materials studied in the (000) Brillouin zone the appropriate G is

$$G(\vec{q}, \omega) = \frac{1}{2} [G^{+-}(\vec{q}, \omega) + G^{-+}(\vec{q}, \omega)] + G^{zz}(\vec{q}, \omega) \quad (37)$$

which simplifies to

$$G(\vec{q}, \omega) = 3G^{zz}(\vec{q}, \omega) \quad (38)$$

in the paramagnetic phase since $g^{+-} = 2g^{zz}$.

III. RELATION TO OTHER THEORIES

The dynamical susceptibility theory described in Sec. II is an improvement on the singlet-triplet and similar models in that spin waves between all levels of the ground multiplet are included. Even at $T=0$, where the excited states are not populated, the theory gives different results from the singlet-triplet model since it is found to predict a zone-center energy gap in agreement with the experimental results on TbSb (Ref. 5) and the results for Pr₃Tl (Ref. 6) extrapolated to $q=0$. In this $T=0$ limit the theory is shown below to be equivalent to conventional pseudoboson theory as might be expected since the intensity of all the excited-state

spin waves tends to zero as the population factors for each excited level approach zero.

For all finite temperatures the present theory gives results that were not previously available. The inclusion of excited-state spin waves, in particular the $\Gamma_4-\Gamma_3$ spin waves, greatly affects the predicted temperature dependence of the spectrum.

In the paramagnetic phase the theory becomes equivalent to the theory of Fulde and Peschel¹⁵ as shown below. The use of more realistic model parameters¹⁶ in the present theory leads to better agreement with experiment than was found by Peschel *et al.*²⁰ in their model calculation for Pr₃Tl.

There are also similarities with the theory of spin waves in itinerant magnets as discussed in Sec. III C.

A. Relation to pseudoboson theory

For transverse spin waves the single-ion susceptibility at $T=0$ becomes

$$g^{+-}(\omega) = \sum_n \left(\frac{S_{+0n} S_{-0n}}{\omega - \omega_{n0}} - \frac{S_{+n0} S_{-n0}}{\omega + \omega_{n0}} \right). \quad (39)$$

In pseudoboson theory the response functions are

$$P^{+-}(nm, ij, t) = -i\Theta(t) \langle [a_n^\dagger(it), a_m(j0)] \rangle, \quad (40)$$

where $a_n^\dagger = C_n^\dagger C_0$ with similar expressions for the related functions P^{-+} , P^{++} , and P^{--} . The Heisenberg equation of motion for the P^{+-} operators in a ferromagnetic system can be obtained after evaluating the commutator of a_n^\dagger with the transverse part of the Hamiltonian expressed in pseudoboson operators as given by Buyers *et al.*,¹³ Eq. (17):

$$\begin{aligned} \sum_{n'} (\omega + \omega_{n0}) P^{+-}(n'n'', \vec{q}\omega) \\ = -\delta_{nn''} - \sum_{n'} A_{nn'} P^{+-}(n'n'', \vec{q}\omega) \\ - \sum_{n'} B_{nn'} P^{--}(n'n'', \vec{q}\omega), \end{aligned} \quad (41)$$

where

$$A_{nn'} = J(\vec{q}) (S_{-n0} S_{+0n'} + S_{+n0} S_{-0n'})$$

and

$$B_{nn'} = J(\vec{q}) (S_{+n0} S_{-n'0} + S_{-n0} S_{+n'0}). \quad (42)$$

In an obvious matrix notation, Eq. (41) and the related equations are

$$\begin{aligned} (\omega \underline{1} + \omega_0) \cdot \underline{P}^{+-} &= -\underline{1} - \underline{A} \cdot \underline{P}^{+-} - \underline{B} \cdot \underline{P}^{--}, \\ (\omega \underline{1} - \omega_0) \cdot \underline{P}^{--} &= \underline{0} + \underline{A} \cdot \underline{P}^{--} + \underline{B} \cdot \underline{P}^{+-}, \\ (\omega \underline{1} - \omega_0) \cdot \underline{P}^{-+} &= \underline{1} + \underline{A} \cdot \underline{P}^{-+} + \underline{B} \cdot \underline{P}^{++}, \\ (\omega \underline{1} + \omega_0) \cdot \underline{P}^{++} &= \underline{0} - \underline{A} \cdot \underline{P}^{++} - \underline{B} \cdot \underline{P}^{-+}. \end{aligned} \quad (43)$$

To compare with the dynamical susceptibility the-

ory we evaluate the pseudoboson response G_P^{+-} by substituting in Eq. (18) the pseudoboson transformation

$$S_+ = \sum_n S_{+0n} a_n + \sum_n S_{+n0} a_n^\dagger. \quad (44)$$

The result is

$$G_P^{+-}(\vec{q}, \omega) = \sum_{nn'} [S_{+0n} S_{-0n'} P^{--}(nn', \vec{q}, \omega) + S_{+0n} S_{-n'0} P^{+-}(nn', \vec{q}, \omega) + S_{+n0} S_{-n'0} P^{++}(nn', \vec{q}, \omega)]. \quad (45)$$

For each nn' component of $P^{\alpha\beta}$ the expression given by Eqs. (43) is substituted in (45) producing a series of energy denominators of the form $\omega + \omega_{n0}$. After a certain amount of algebra (45) becomes

$$G_P^{+-}(\vec{q}, \omega) = g^{+-}(\omega) + J(\vec{q}) g^{+-}(\omega) G_P^{+-}(\vec{q}, \omega) \quad (46)$$

with $g^{+-}(\omega)$ given by its low temperature limit, Eq. (39). Since (46) is equivalent to (32) we have $G_P = G$ and thus the dynamical susceptibility theory reduces to pseudoboson theory at $T=0$. A similar equivalence exists for the longitudinal spin waves.

B. Dynamical susceptibility in the paramagnetic phase

In the paramagnetic phase $\langle S_z \rangle = 0$ and there is no distinction between the longitudinal and transverse response functions, (32) and (33). The special relations between the matrix elements that exist when $\langle S_z \rangle = 0$, such as those between the triplet Γ_4 (states 2, 3, 4) and the ground singlet Γ_1 (state 1),

$$\langle S_{z21} \rangle^2 = 2 \langle S_{z31} \rangle^2, \quad (47)$$

then conspire to ensure that

$$g^{+-}(\omega) = 2g^{zz}(\omega). \quad (48)$$

To obtain an equation for the total susceptibility, the single-ion part is first written

$$g(\vec{S} \cdot \vec{S}, \omega) \equiv \frac{1}{2} g^{+-}(\omega) + \frac{1}{2} g^{-+}(\omega) + g^{zz}(\omega). \quad (49)$$

Each term is then rewritten in the form

$$g^{+-}(\omega) = \sum_{mn} f_m \left(\frac{S_{+mn} S_{-nm}}{\omega - \omega_{mn}} - \frac{S_{+nm} S_{-mn}}{\omega - \omega_{nm}} \right), \quad (50)$$

which leads to

$$g(\vec{S} \cdot \vec{S}, \omega) = \sum_{mn} \frac{\omega_{mn}}{\omega^2 - \omega_{nm}^2} (f_m - f_n) + \left(\frac{1}{2} S_{+mn} S_{-nm} + \frac{1}{2} S_{-mn} S_{+nm} + S_{zmn} S_{znm} \right) = \sum_{mn} \frac{\omega_{mn}}{\omega^2 - \omega_{nm}^2} (f_m - f_n) |\vec{S}_n^m|^2 \quad (51)$$

using the special properties of the matrix elements (48). Equation (51) is the same as the single-ion susceptibility of the paramagnetic phase given by

Fulde and Peschel,¹⁵ who used a diagram technique to derive their result. The total susceptibility $G(\vec{S} \cdot \vec{S}, \vec{q}, \omega)$ is also equivalent to Fulde and Peschel's result in the paramagnetic phase because the single-ion susceptibilities, of both theories, renormalize in the same way with $J(\vec{q})$.

C. Relation to magnetism in metals

In the theory of itinerant ferromagnetism (see, e.g., Cooke¹⁹ and references therein) the appropriate equation of motion is that of the total spin operator $\vec{S}(\vec{r})$ regarded as a continuous function of position \vec{r} . Its relationship to the localized spin operators, $\vec{S}(i)$, used in this paper will now be described.

The component of the total spin operator, $S_+(\vec{r})$, can be expressed¹⁹ in terms of the Fermi operators $C_n(\vec{k})$ that annihilate an electron of wave vector \vec{k} and index n whose wave function is $\psi_{n\vec{k}}(\vec{r})$:

$$S_+(\vec{r}) = \sum_{nn'} \sum_{\vec{k}\vec{k}'} \psi_{n'\vec{k}'}^\dagger(\vec{r}) \times S_+ \psi_{n\vec{k}}(\vec{r}) C_n^\dagger(\vec{k}') C_n(\vec{k}). \quad (52)$$

The index n is here taken to be a combined index for the band and spin. To make connection with the localized-spin picture the wave functions are written in tight-binding form

$$\psi_{n\vec{k}}(\vec{r}) = \sum_i \psi_n(\vec{r} - \vec{i}) e^{i\vec{k} \cdot \vec{i}}, \quad (53)$$

where the $\psi_n(\vec{r} - \vec{i})$ is an atomic orbital localized in cell \vec{i} . The total spin operator (52) is then integrated over a cell to give the localized spin operator for nonoverlapping atomic orbitals as

$$S_+(i) = \int_{V_i=V_a} S_+(r) dr = \sum_{nn'} S_{+n'n}(i) C_n^\dagger(i) C_n(i) \quad (54)$$

with

$$S_{+n'n}(i) = \int_{V_a} \psi_{n'}^\dagger(\vec{r}) S_+ \psi_n(\vec{r}) d^3 r \equiv \langle n' | S_+ | n \rangle \quad (55)$$

and the localized annihilation operators related to the itinerant ones by

$$C_n(i) = \sum_{\vec{k}} C_n(\vec{k}) e^{+i\vec{k} \cdot \vec{i}}. \quad (56)$$

Thus the itinerant spin operators go over into the localized ones in the limit of localized magnetic orbitals provided the identification is made of n , the band and spin index, with the index n of the single-ion levels at site i . The localized operators of the present theory thus differ from the one-electron operators that are usual in the band theory of magnetism. They annihilate or create a state $|n\rangle$ in which the Hund's rule correlation of the electrons is already included. The states $|n\rangle$ are the states within the cubic-field ground state in the

case of transition-metal ions, and the spin-orbit ground state $J=L \pm S$ in the case of rare-earth ions.

The decoupling procedure used in Sec. IIB to truncate the hierarchy of equations is the generalized random-phase approximation as given, for example, by Cooke¹⁹:

$$C_1^\dagger C_2^\dagger C_3 C_4 = f_1(\delta_{1,4} C_2^\dagger C_3 - \delta_{1,3} C_2^\dagger C_4) + f_2(\delta_{2,3} C_1^\dagger C_4 - \delta_{2,4} C_1^\dagger C_3), \quad (57)$$

where in the present case "1" represents index n and site i . Because the exchange in insulators couples ions only on different sites, the form that arose in Sec. IIB was special in having $i \neq l$ so that $1=3$ and $2=4$ are not allowed. Thus

$$\begin{aligned} C_m^\dagger(i) C_s(i) C_q^\dagger(l) C_p(l) &= C_m^\dagger(i) C_q^\dagger(l) C_p(l) C_s(i) \\ &= f_m(i) \delta_{ms} C_q^\dagger(l) C_p(l) \\ &\quad + f_q \delta_{pq} C_m^\dagger(i) C_s(i) \end{aligned} \quad (58)$$

as stated in Sec. IIB.

IV. RESULTS

The spectrum of magnetic excitations in Pr_3Tl has been obtained numerically as a function of temperature from the dynamical susceptibility theory of Sec. III. The crystal-field parameters and the nearest-neighbor exchange constant were the same as those of Paper I¹⁶ which were chosen to be consistent with the observed $T=0$ spin-wave energy at the zone boundary,⁷ i. e., a splitting $\Delta = 77$ K, and with the ordered moment of $0.75\mu_B$.

The poles of $G^{+-}(\vec{q}, \omega)$ and $G^{zz}(\vec{q}, \omega)$, Eqs. (32) and (33), give the frequencies of the spin waves. The poles of $G(\vec{q}, \omega)$ are conventionally obtained by diagonalizing a matrix. For finite temperature the dynamical susceptibility matrix, given by Eq. (29), is of order $2S(2S+1)$, larger than the matrix of the pseudoboson theory since excitations between all pairs of levels are possible. For Pr^{3+} with $S=4$ this is not an impossibly large matrix to diagonalize, particularly if the factorization into longitudinal and transverse parts is utilized. Fortunately there is a much simpler way to obtain the solution when numerical solutions are sought and this is the method we have adopted.

The method is simply to search for peaks in $\text{Im} G(\vec{q}, \omega + i\epsilon)$ as a function of frequency at constant \vec{q} as is done experimentally. The steps in $\text{Re}\omega$ are less than ϵ while ϵ is chosen small compared with the intermode spacing so that no peaks are missed. Typically $\epsilon = 0.002$ THz is set in an initial search and once a peak is found ϵ is reduced to a small value (0.0001) and the peak located to six-figure accuracy. This method is found to be comparable in speed to diagonalizing a matrix and has the advantage that the intensities of the spin waves are found at the same time without having

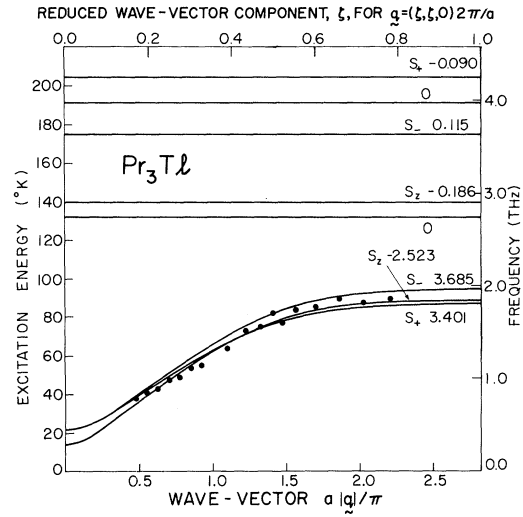


FIG. 1. Dispersion relation of spin waves propagating along the [110] direction of Pr_3Tl at $T=0$. The full circles are the experimental results of Birgeneau *et al.* (Ref. 6). The single-ion matrix elements corresponding to each transition $0 \rightarrow n$ are $S_\alpha \equiv \langle n | S_\alpha | 0 \rangle$, where $\alpha = +, -, \text{ or } z$.

to evaluate eigenvectors. Since the peaks are Lorentzian the intensity is proportional to the value of $\text{Im} G(\vec{q}, \omega)$ at the peak times 2ϵ .

The dispersion relations for Pr_3Tl at $T=0$ are shown in Fig. 1. The choice of the $[\zeta\zeta 0]$ direction for the wave vector closely simulates⁷ the response expected for a polycrystal at the same $|\vec{Q}|$. For the present nearest-neighbor model the frequencies of the excitations with the same $|\vec{Q}|$ are found to be isotropic to 0.3%. Only the three lowest branches of Fig. 1 have appreciable dispersion. The higher-frequency branches, since they have small matrix elements, are almost independent of wave vector as expected from Eq. (32) or (33).

At finite temperatures the excited states become populated and new modes appear. At $0.901T_C$ the dispersion relations of the lowest frequency excitations are as shown in Fig. 2. The new branch of excited-state spin waves in the vicinity of 1.2 THz interacts strongly with the main $\Gamma_4-\Gamma_1$ branch. Greater detail of the transverse modes in the region of the interaction is shown in Fig. 3 and in the Appendix a method is given for finding out which modes can cross.

In Fig. 2 the new branches are weak, as indicated by the symbols, W , except for three modes out of the six expected between the three Γ_4 levels (2, 3 and 4) and the two Γ_3 levels (5 and 6). The relatively strong excited-state branches are the longitudinal mode 6-3 and the transverse modes 5-2 and 5-4. Mode 5-3 is magnetic dipole inactive whereas 6-4 and 6-2 are weaker than the others by

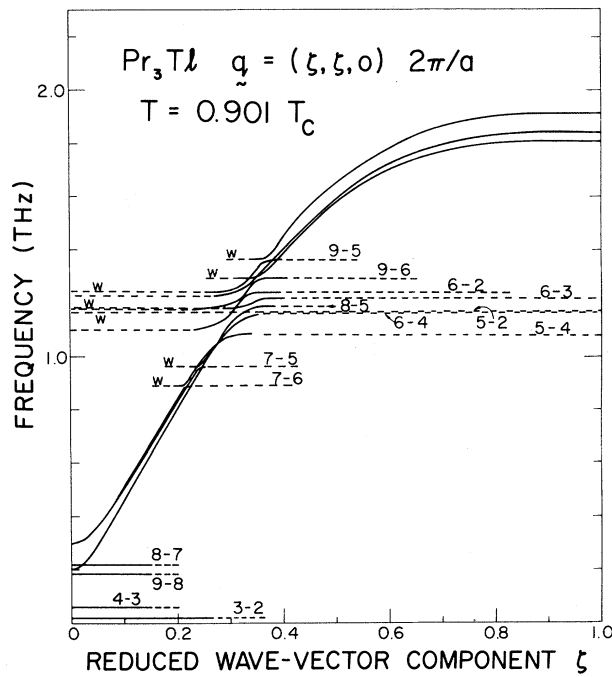


FIG. 2. Dispersion relation for Pr_3Tl at finite temperature. The symbols $m-n$ identify the single-ion transitions corresponding to the excited-state spin waves.

a factor of ~ 4 . These and other relations can be found from the level diagram and matrix elements in Fig. 4. The lowest-lying modes within the triplets Γ_4 (3-2 and 4-3) and Γ_5 (9-8 and 8-7) exhibit an energy gap at $\vec{q}=0$. This is to be contrasted with the Goldstone (or acoustic) modes that occur in the singlet-triplet model (see Smith,¹⁰ for ex-

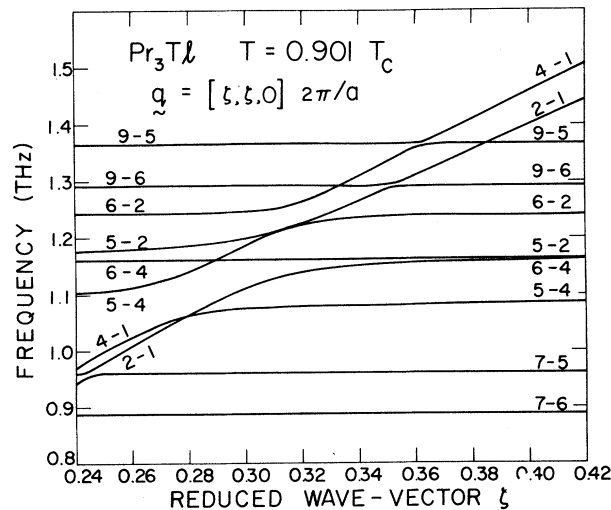
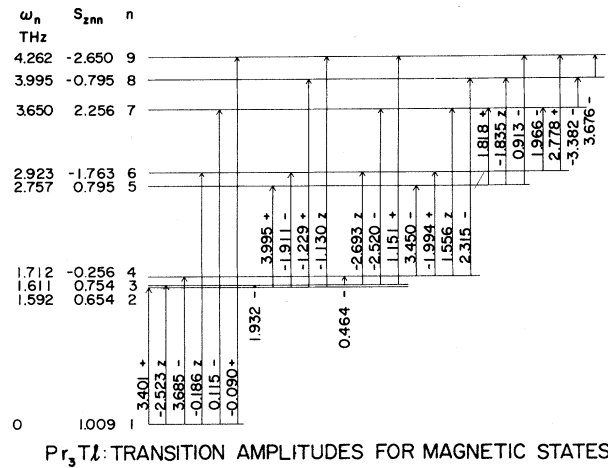


FIG. 3. Details of the crossing and anticrossing for transverse modes only.



Pr_3Tl : TRANSITION AMPLITUDES FOR MAGNETIC STATES

FIG. 4. Energy levels of the Pr^{3+} ion in the crystal-line field and molecular field appropriate to Pr_3Tl at $T=0$. On each transition is given the appropriate matrix element $\langle m | S_\alpha | n \rangle$ and a symbol α indicating whether the transition is S_x , S_y , or S_z .

ample). The gap is a result of the inclusion of higher excited states than Γ_4 .

The intensity of the Γ_3 - Γ_4 modes is anomalously large near the crossover. The intensity, for no interaction with other modes, depends on

$$f_n(\Gamma_4) - f_m(\Gamma_3),$$

where n belongs to the exchange split Γ_4 group of levels and m to Γ_3 . Approximately 0.7% of the population is in each of the Γ_4 levels while the $f_m(\Gamma_3)$ are two orders of magnitude smaller. Since the dominant Γ_3 - Γ_4 matrix elements are comparable with the Γ_4 - Γ_1 matrix elements, in the single-ion approximation the Γ_3 - Γ_4 modes should have only $\sim 0.7\%$ of the intensity of the Γ_4 - Γ_1 modes. Near the crossover this is no longer the case as shown in Fig. 5 which gives the neutron scattering that would be measured at $(0.25, 0.25, 0)2\pi/a$ with a spectrometer of small resolution width. Fulde and Peschel¹⁵ noted similar behavior in their calculations for the paramagnetic phase. Some of the large intensity of the lower Γ_4 - Γ_1 branches, e.g., the 2-1 transition, proportional to $(f_1 - f_2)(S_{+21})^2$ with $f_1 \sim 0.99$, is transferred to the weak Γ_3 - Γ_4 branches. The mixing of branches becomes increasingly strong as the crossover is approached.

There has been much discussion of the nature of the soft mode in singlet-ground-state systems. The behavior of the zone-center modes as a function of temperature is shown in the lower part of Fig. 6. A schematic energy level diagram is superposed as an aid in identifying the various modes. The pair of levels indicated on each mode indicates only the transition that makes the largest

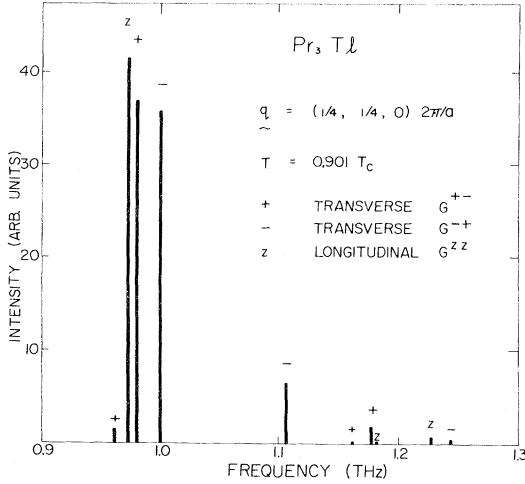


FIG. 5. Neutron scattering for \vec{q} just less than the crossover wave vector as observed with a spectrometer of very high resolution.

contribution to the mode wave function. This identification is only qualitative in view of the mixing discussed in the last paragraph, but is given as an aid in understanding the physical process. The two transverse zone-center modes are plotted as a single line as they are almost degenerate. Their frequency falls by a factor of ~ 6 and remains finite when $T \rightarrow T_c$. The single longitudinal (S_z) mode falls by a factor of ~ 4 and becomes degenerate with the transverse modes as it must in the paramagnetic phase.

The main branch, identified as $\Gamma_4 - \Gamma_1$ at low temperature, does not go soft. Instead new transverse modes of very low frequency appear that do go soft at the transition. In Fig. 6 their frequencies have been plotted for $T > 0.6 T_c$ where the intensity becomes appreciable. They are associated with the transitions 3-2 and 4-3 within the Γ_4 triplet, and since they have the same symmetry as the transverse $\Gamma_4 - \Gamma_1$ modes (see Appendix) they interact within them. One may say that the $\Gamma_4 - \Gamma_1$ modes "drive" the low-frequency modes within the triplet soft, or that the presence of the low-frequency modes "prevents" the $\Gamma_4 - \Gamma_1$ branch from going soft, but this is largely a pictorial way of speaking. As emphasized above the transitions are mixed together by the exchange.

Several modes are not shown in Fig. 6, including two soft quadrupolar modes: the mode within the Γ_3 doublet and the 4-2 mode. Note that Smith¹⁰ plots the 4-2 mode although it has zero magnetic dipole strength. The soft modes within the Γ_5 triplet are of very low intensity, as are several higher-frequency modes which are likewise not shown. There are 27 magnetic dipole modes in all.

It is incorrect to identify the transverse modes

within the triplet as the soft modes that are responsible for the transition, since Smith¹⁰ has pointed out that they do not have the correct symmetry. According to Smith the true soft modes have zero frequency at all temperatures and increase in intensity as required to make the longitudinal susceptibility diverge as $T \rightarrow T_c$. Our numerical calculations indeed show that the transverse susceptibility does diverge as $T \rightarrow T_c$, but the longitudinal susceptibility does not.²⁶ This is because the modes whose frequency goes to zero at T_c and which carry a finite magnetic dipole strength are all transverse modes. The truly elastic response of the longitudinal spin components is ignored in the present RPA theory and would, if included in a better theory, make the longitudinal susceptibility diverge also.²⁶ A theory that is consistent with the hydrodynamic behavior is the long-time approximation of Mori.²¹ It has been applied to spin waves by Cheung²² but only to the idealized singlet-singlet problem.

The temperature dependence of the modes of wave vector $(\frac{1}{4}, \frac{1}{4}, 0)2\pi/a$ is shown in Fig. 6. Here

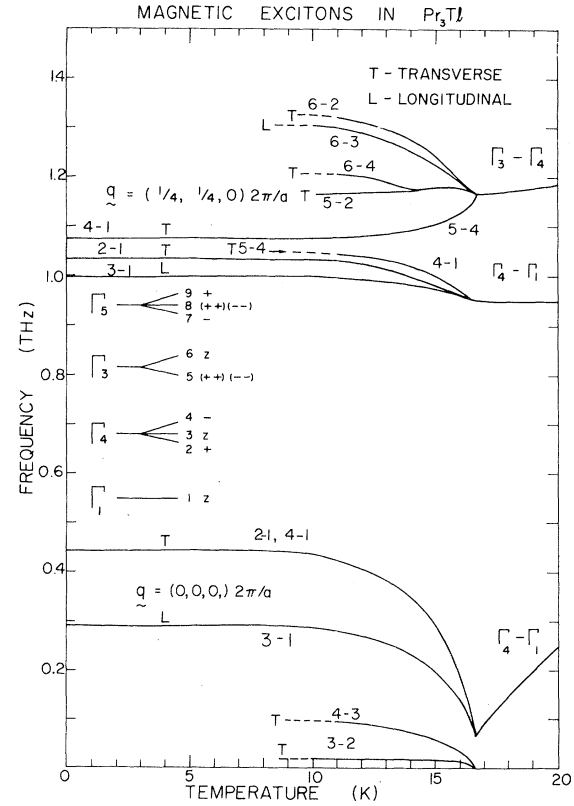


FIG. 6. Temperature dependence of the spin waves. The zone-center spin waves (lower part of figure) are compared with those at small but finite wave vector (upper part of figure). The schematic level scheme at left is a key to the mode labeling.

the behavior is more complex. One simple result emerges; the percentage change in frequency of these modes is much less than that of the zone-center modes. Further, since one group of modes moves to lower frequencies and the other to higher frequencies as the temperature is raised, it is expected that, when viewed with a spectrometer whose resolution spans the mode frequencies, little variation with temperature will be observed.

It is clear from the results already presented that the magnetic excitations in Pr_3Tl are considerably more complex than is suggested by the initial results of Birgeneau *et al.*^{6,7} who plotted a one-branch "dispersion relation." The interpretation of this curve must certainly be that it is the neutron peak position, ω , versus wave vector rather than a dispersion relation for any branch of excitations. The experimental resolution was sufficiently coarse that the neutron peak position can be an average not only over the components of a given transition, e.g., the three $\Gamma_4-\Gamma_1$ excitations, but also over the components of excited-state transitions such as $\Gamma_3-\Gamma_4$. The latter is certainly the case for the large majority of the published results on the temperature variation of the peak position, as the peak studied was at $Q=0.6 \text{ \AA}^{-1}$, i.e., $(0.33, 0.33, 0)2\pi/a$, a wave vector close to the crossover region as can be seen from Fig. 2. To compare with the published neutron peak position the appropriate weighted average frequency has been derived from the results at 0.6 \AA^{-1} :

$$\bar{\omega} = \sum_j \omega_j I_j / I, \quad (59)$$

where

$$I = \sum_j I_j.$$

The position of each peak in the neutron scattering $S(0.6, \omega)$, Eq. (35), is ω_j , and I_j is the intensity at the peak. For several temperatures where there were many closely spaced peaks the neutron peak position was also computed as

$$\bar{\omega} = \frac{\sum_{\omega} \omega S(\vec{Q}, \omega)}{\sum_{\omega} S(\vec{Q}, \omega)}, \quad (60)$$

where the sum was made over a constant wide range encompassing the range of interest and the steps in ω were equal to $\text{Im}\omega$. In general the two methods agreed to within 0.1% but for certain temperatures where the mode density was high, differences as large as 1% were obtained in which case the improved expression (60) was used. The temperature dependence of the total intensity I was also obtained at the same time.

The theoretical results for the temperature dependence of the neutron peak position and the in-

tegrated intensity of the neutron group are shown in Fig. 7. Also shown are experimental results which were obtained from the line shapes of Fig. 7 in the paper by Birgeneau where $\bar{\omega}$ was taken as the midpoint of the line through the half-height points, and I as the planimeted area under each neutron group when corrected for background. The normalized frequency is plotted so as to remove the small displacement at $T=4.5 \text{ K}$ between the theoretical (1.28 THz) and experimental (1.13 THz) frequency. The predicted frequency of the neutron group remains constant to within 5% of its low-temperature value for all the temperatures studied in the experiment. The error bar on the 4.5-K experimental point is $\pm 5\%$. The width of the neutron group at 4.5 K was of the order of 0.35 THz or about 32% of the frequency of 1.13 THz. Thus the theoretical peak position varies by no more than one sixth of the peak width. It is concluded that theory and experiment are in good agreement for the temperature dependence of the frequency.

The agreement for the temperature variation of the intensity (Fig. 7 lower part) is not so good, but is in qualitative agreement with the observation of a general falloff with temperature. Birgeneau (private communication) has found, in a further experiment at Brookhaven with higher resolution, that the falloff in intensity was slower and that structure was observed in the neutron group measured near the predicted $\Gamma_4-\Gamma_1$, $\Gamma_3-\Gamma_4$ crossover. The intensity below T_c is nearly constant on our model for the 0.6-\AA^{-1} wave vector of Fig. 7, apart from a readjustment near T_c where the population factors

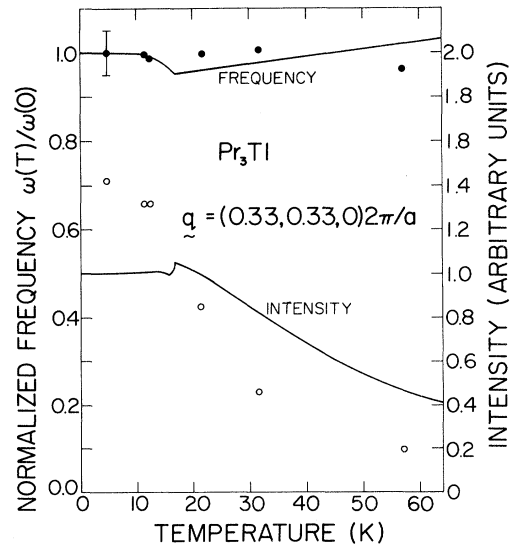


FIG. 7. Temperature dependence of the frequency (left scale) and intensity (right scale) of the peak in the neutron scattering compared with the experimental results (full and open circles) of Birgeneau (Ref. 7).

and matrix elements for the many transitions that contribute are changing rapidly.

The transition temperature predicted by the theory is 16.65 K whereas that observed is 11.3 ± 0.3 K. The discrepancy is largely the result of the use of molecular-field theory to calculate $\langle S_z \rangle$. It could be argued, however, that a better model would have resulted if the exchange constant had been chosen to fit T_C rather than the observed spontaneous moment of $0.75\mu_B$. This would have resulted in an improved agreement with the observed frequency (1.13 THz) of the peak at $T=4.5$ K and $Q=0.6 \text{ \AA}^{-1}$. With a better theory (as opposed to better parameters), however, both methods should agree.

We conclude that the dynamical susceptibility theory developed in this and in paper I gives a reasonable description of the spin waves in complex magnetic systems. It reproduces many of the features of the spectrum of the singlet-ground-state ferromagnet Pr_3Tl both in the pure state and when diluted with La.²³ The theory predicts an energy gap for all $T < T_C$ in contrast with the singlet-triplet model. The transverse modes within the triplet and not the main $\Gamma_1-\Gamma_4$ modes go soft as $T \rightarrow T_C$. The absence of a soft longitudinal mode is not understood²⁶ but is in agreement with the work of Smith.¹⁰ The theory contains the basic physics required to describe excited-state spin waves and any mode-mode interaction that may occur and is applicable at all temperatures. Since it involves a generalized random-phase approximation, the theory cannot describe effects of fluctuations or critical effects. The theory is of such a form, however, that it should be possible to extend it to include some of the effects of fluctuations, e.g., linewidths, and it is hoped to perform such an extension in the future.

Note added in proof. The divergence of the central mode arising from the elastic transitions, $m=n$ in Eq. (30), is discussed by M. E. Lines [J. Phys. C7, L282 (1974)] for the singlet-triplet model, and is generalized to the full-level scheme of Pr_3Tl by W. J. L. Buyers [AIP Conf. Proc. (to be published)].

ACKNOWLEDGMENTS

The authors have had useful discussions with S. R. P. Smith, B. R. Cooper, and R. J. Birgeneau.

APPENDIX

The conditions under which two modes can cross in $\omega - \vec{q}$ space are discussed in what follows, and the classification of the levels according to symmetry is described.

We note first that the longitudinal modes, de-

scribed by G^{zz} , can cross the transverse modes, described by G^{+-} or G^{-+} , since Eq. (31) shows they are orthogonal as a result of $g^{z-}=0$ and $g^{z+}=0$. The transverse modes satisfy two equations of the form of Eq. (32) with $G=G^{+-}$ and $G=G^{-+}$, respectively, indicating that there are two types of transverse modes. The first type satisfies Eq. (29) with $G^{+-}(mn\vec{q}\omega) \equiv S_{+mn} \hat{G}^-(mn\vec{q}\omega)$:

$$(\omega - \omega_n + \omega_m)G^{+-}(mn\vec{q}\omega) = (f_m - f_n) |S_{-mn}|^2 + (f_m - f_n) |S_{-mn}|^2 J(\vec{q}) \sum_{pq} G^{+-}(qp, \vec{q}\omega). \quad (\text{A1})$$

This shows that the single-ion transition, $m-n$, that is characterized by matrix element S_{-mn} and occurs at $\omega = \omega_n - \omega_m$, couples to all other transitions $q \rightarrow p$, characterized by matrix element S_{-qp} and frequencies $\omega = \omega_p - \omega_q$. It does not couple to transitions characterized by S_{+qp} . Thus the "S₋" transitions are orthogonal for this system to the "S₊" transitions. They would not be orthogonal in a system like CoF_2 where both S_{+qp} and S_{-qp} are nonzero for any one transition $p \rightarrow q$. It may be argued that in (A1) the energy loss transitions $p \rightarrow q$, where $\omega_p > \omega_q$, are really "S₊" transitions since $S_{-pq} = S_{+qp}$. However, their response occurs at negative frequencies, $\omega = -(\omega_p - \omega_q)$, and so is always off-resonance as far as the positive frequency transition, $\omega = \omega_n - \omega_m$, is concerned. These negative frequency transitions can therefore never affect any anticrossing at positive frequencies. Notwithstanding their inability to provide mode-mode repulsion, they do, of course, mix in and change the position of the positive frequency poles by a small amount.

The above ideas are illustrated by the theoretical results of Fig. 2 which shows the complex network of interacting transverse modes in the region of the crossover. Comparison with the transition matrix elements of Fig. 4 confirms that allowed crossings consist of an intersection between an "S₊" and an "S₋" mode. Any "S₊" mode is in general a mixture of the transitions

1-2, 1-9, 2-5, 2-8, 3-9, 4-6, 5-7, 6-9, while any "S₋" mode contains

$$1-4, 1-7, 2-3, 2-6, 3-4, 3-7, 4-5, 4-8, 5-9, 6-7, 7-8, 8-9.$$

From the transition matrix elements we can classify the level symmetry in a qualitative way by observing how each level is connected to each adjacent level. Thus, since level 2 is obtained from the ground state by the spin-raising operator S_+ , we may call level 2 a level of + symmetry. Likewise levels 3 and 4 are of z and - symmetry, respectively. Level 5 is connected by S_+ to level 2 which has already been created by one spin-raising

ing operation. We describe this contribution to level 5 by $(++)$. Level 5 can also be obtained from 4 by S_z giving $(--)$ in all. Level 5 is therefore denoted $(++) + (--)$. Since it departs by two magnetic-dipole operators from the ground state we anticipate that the $1 \rightarrow 5$ transition is quadrupolar in character and is absent as a magnetic-dipole transition as indeed it is ($S_{\alpha 51} = 0$ from Fig. 4). However, transitions from 5 to levels of symmetry $+$ or $-$ will be allowed since this involves only one magnetic-dipole operator. Thus S_{+75} is finite since level 7 is a $-$ level (S_{-71} finite). Note that the sym-

metry of a level, say 7, can be inferred independently of the route followed from the ground state. Thus 7 from the route $1 \rightarrow 3 \rightarrow 7$ is $(z) \times (-) = (-)$ since S_z does not change the symmetry, from $1 \rightarrow 4 \rightarrow 7$ is $(-) \times (z) = (-)$, and from $1 \rightarrow 6 \rightarrow 7$ is $(z) \times (-) = (-)$. The resulting symmetry labels are attached to the schematic level scheme on the left-hand side of Fig. 6. It is found that the same symmetry labels apply in the disordered phase as may be seen from Table I of Paper I¹⁶ provided the identity of the various components of degenerate crystal-field levels is maintained.

*Present address: University of Montreal, Computer Science Department, Montreal.

¹G. T. Trammell, Phys. Rev. **131**, 932 (1963).

²B. Bleaney, Proc. R. Soc. A **276**, 19 (1963).

³H. R. Child, M. Wilkinson, J. W. Cable, W. C. Koehler, and E. O. Wollan, Phys. Rev. **131**, 922 (1963).

⁴B. R. Cooper and O. Vogt, J. Phys. **32**, C1-958 (1971).
Y. L. Wang and B. R. Cooper, Phys. Rev. **185**, 696 (1969).

⁵T. M. Holden, E. C. Svensson, W. J. L. Buyers, and O. Vogt, *Neutron Inelastic Scattering*, (IAEA, Vienna, 1972), p. 553; also T. M. Holden, E. C. Svensson, W. J. L. Buyers, and O. Vogt, Phys. Rev. B (to be published).

⁶R. J. Birgeneau, J. Als-Nielsen, and E. Bucher, Phys. Rev. Lett. **27**, 1630 (1971). R. J. Birgeneau, J. Als-Nielsen, and E. Bucher, Phys. Rev. B **6**, 2724 (1972).

⁷R. J. Birgeneau, AIP Conf. Proc. **10**, 1664 (1973).

⁸D. A. Pink, J. Phys. C **1**, 1246 (1968).

⁹Y. Y. Hsieh and M. Blume, Phys. Rev. B **6**, 2684 (1972).

¹⁰S. R. P. Smith, J. Phys. C **5**, L157 (1972).

¹¹B. R. Cooper, Phys. Rev. B **6**, 2730 (1972).

¹²B. Grover, Phys. Rev. **140**, A1944 (1965).

¹³W. J. L. Buyers, T. M. Holden, E. C. Svensson, R. A. Cowley, and M. T. Hutchings, J. Phys. C **4**, 2139 (1971). This paper gives specific expressions for the pseudoboson secular determinant that are applicable to any many-level system.

¹⁴P. Martel, R. A. Cowley, and R. W. H. Stevenson, Can. J. Phys. **46**, 1355 (1968).

¹⁵P. Fulde and I. Peschel, Z. Phys. **241**, 82 (1971).

We are grateful to P. Fulde for drawing our attention to similar work by M. Klenin and I. Peschel, Phys. Kondens. Materie **16**, 219 (1973). They reach similar conclusions about the soft-mode behavior of Pr₃Tl but do not perform realistic numerical calculations for comparison with experiment.

¹⁶T. M. Holden and W. J. L. Buyers, Phys. Rev. B **9**, 3797 (1974), referred to as Paper I.

¹⁷M. T. Hutchings, Solid State Phys. **16**, 227 (1964).

¹⁸R. A. Cowley, W. J. L. Buyers, P. Martel, and R. W. H. Stevenson, J. Phys. C **6**, 2997 (1973).

¹⁹J. F. Cooke, Phys. Rev. B **7**, 1108 (1973).

²⁰I. Peschel, M. Klenin, and P. Fulde, J. Phys. C **5**, L194 (1972).

²¹H. Mori, Prog. Theoret. Phys. (Kyoto) **33**, 423 (1965).

²²T. H. Cheung, Phys. Status Solidi B **58**, 567 (1973).

²³Reference 16 gives the results for Pr₃Tl doped with 12-at.% La and the results of the theory for 7-at.% La doping will be found in a forthcoming paper by J. Kjems, R. J. Birgeneau, E. Bucher, M. E. Lines, and W. J. L. Buyers.

²⁴For a proof see M. Blume and R. J. Birgeneau, J. Phys. C **7**, L282 (1974).

²⁵This is because Eq. (29) becomes an identity for $\omega = 0$ and $m = 12$. The elastic terms can, however, be included if the limit $m \rightarrow n$ is taken carefully (see Note added in proof).

²⁶See Note added in proof.